Contents lists available at ScienceDirect

Journal of South American Earth Sciences

journal homepage: www.elsevier.com/locate/jsames

A screening approach for selecting fossils for molecular analysis

Damián A. Ibarra [a,b], Luciano Brambilla [a,c,d,e,*], Pablo Straccia [f], Rubén D. Scian [f], Lucas R. Brun [a,b]

[a] Laboratorio de Biología Ósea, Facultad de Ciencias Médicas, Universidad Nacional de Rosario, Santa Fe, Argentina
[b] Consejo Nacional de Investigaciones Científicas y Técnicas (CONICET), Buenos Aires, Argentina
[c] Facultad de Ciencias Bioquímicas y Farmacéuticas, Universidad Nacional de Rosario, Suipacha 531, S2002LRK, Rosario, Argentina
[d] Consejo de Investigaciones de la Universidad Nacional de Rosario (CIUNR), Rosario, Argentina
[e] Centro de Estudios Interdisciplinarios UNR, Maipú 1065, S2000CGK, Rosario, Argentina
[f] Museo Municipal de Ciencias Naturales Pachamama, Niza 1065, Santa Clara del Mar, B7609, Buenos Aires, Argentina

A B S T R A C T

This study investigates the presence of preserved biological remains in fossils, which could be particularly critical for future studies aimed at understanding the evolutionary history of extinct organisms. We focused on osteoderms from specimens of glipotodonts *Panochthus tuberculatus* and *Glyptodon reticulatus* from the Late Pleistocene of Argentina. Our approach involved sectioning the osteoderms and staining them with Coomassie Blue, a dye with high affinity for proteins. Additional staining techniques included Hematoxylin and eosin (H&E) and Masson's Trichrome Staining on histological sections of the same specimens. Sudan IV staining was also performed to verify the presence of lipids. These methods rapidly detected proteins and lipids and mapped their spatial distribution within the specimens, enabling the selection of samples for further molecular analyses. The findings highlight the potential of these methods to advance evolutionary research and improve our understanding of relationships among extinct species.

1. Introduction

In recent decades, there has been growing interest in the preservation of molecular and tissue integrity in fossils and subfossils of vertebrates. Biomolecules, tissues, and cells have been successfully recovered from bone remains dating back to the Mesozoic and Cenozoic (e.g. Schweitzer et al., 2007a, 2007b, 2009, 2013; San Antonio et al., 2011; Cadena and Schweitzer, 2012, Boatman et al., 2014, 2019). The strong interest in the possibility of identifying original organic remains in fossils has prompted the need for novel and practical methods to assess whether a specimen has the potential to yield original biomolecules for subsequent analyses (Anderson, 2022), as well as to differentiate between endogenous and exogenous sources of biological information (Colleary et al., 2022).

In this context, Anderson (2022) proposed two methods as proxies for biomolecule recovery from fossil surfaces: ToF-SIMS mass spectrometry and Raman spectroscopy. While both methods offer high chemical sensitivity, enabling the identification of molecular composition (Raman) or elemental/isotopic composition (ToF-SIMS), they are limited to analyzing very small areas of the fossil, typically ranging from μm^2 to mm^2. This restriction may lead to inaccurate conclusions about the presence of original organic material due to the heterogeneity between preserved and non-preserved regions. Another significant drawback of these methods is their reliance on specialized instrumentation, highlighting the critical need for techniques that can be easily implemented in laboratories aiming to investigate the presence of original organic material.

Cingulates are among the most characteristic groups of the Cenozoic in South America, yet little effort has been devoted to exploring the presence of biological remains in their fossils; however, numerous paleohistological characterizations and comparisons have been conducted using sections of their osteoderms (Hill, 2006; Wolf et al., 2012; Da Costa Pereira et al., 2012; Asakura et al., 2017; Luna et al., 2018). Histologically, osteoderms exhibit a microstructure known as diploe, consisting of a central region of trabecular bone enclosed between an external and an internal layer of compact bone. In both the external and internal layers, collagen fibers are oriented perpendicularly to the surface, whereas in the central region, dominated by trabecular bone, the organization of the fibers becomes less structured (Da Costa Pereira et al., 2012; Wolf et al., 2012). Although these studies have enhanced our understanding of the morphological microstructures of osteoderms, none have employed histological staining, at least in fossil cingulate

This article is part of a special issue entitled: SA Miocene-Pleistocene published in Journal of South American Earth Sciences.

* Corresponding author. Laboratorio de Biología Ósea, Facultad de Ciencias Médicas, Universidad Nacional de Rosario, Santa Fe, Argentina.
E-mail address: lbrambilla@fbioyf.unr.edu.ar (L. Brambilla).

https://doi.org/10.1016/j.jsames.2025.105454
Received 1 December 2024; Received in revised form 13 February 2025; Accepted 24 February 2025
Available online 25 February 2025
0895-9811/

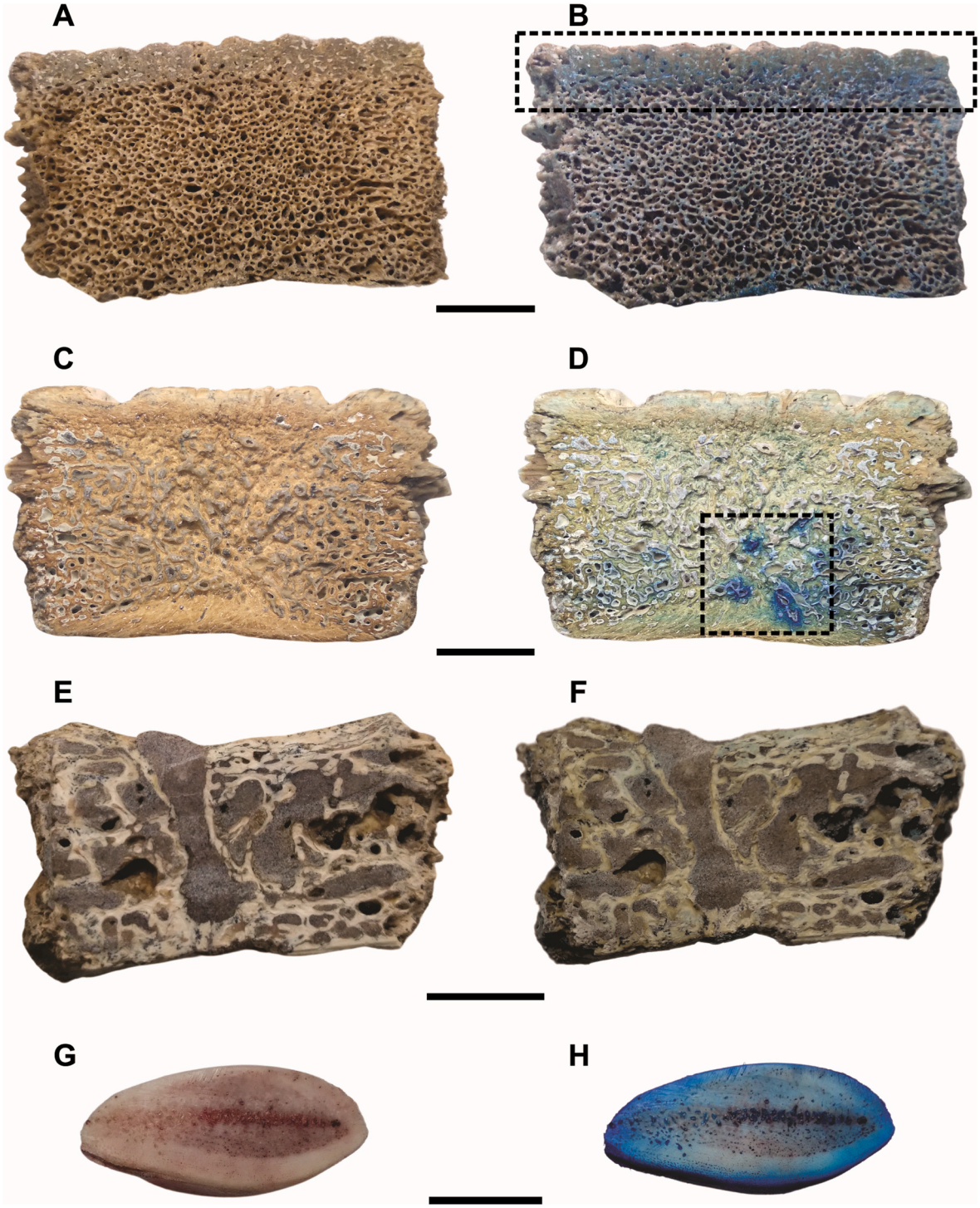

Fig. 1. Coomassie blue staining. Transverse sections, unstained (A, C, E, G) and stained (B, D, F, H). Osteoderm of *P. tuberculatus* MMCNP P2019-07 (A–B); osteoderm of *G. reticulatus* MMCNP P2019-31 (C–D); osteoderm of *Doedicurus clavicaudatus* MLS 500 (E-F, negative control); rib of *Bos taurus* LBO 056 (G-H, positive control). Scale bar = 10 mm. Dashed boxes indicate areas of preserved organic material. (For interpretation of the references to color in this figure legend, the reader is referred to the Web version of this article.)

species. The use of stains, which bind with specificity to tissue structures and impart color, offers an expanded framework for detecting preserved biomolecules, as well as cellular and subcellular structures. At the same time, offers a simpler and more accessible approach to investigating the potential preservation of original biomolecules in fossils.

Among a wide range of stains, Hematoxylin and eosin (H&E) staining remains the most widely used histological technique due to its relative simplicity and effectiveness in vividly highlighting a broad spectrum of tissue structures. Hematoxylin stains cell nuclei blue-black, while eosin imparts shades of pink, orange, and red to the cytoplasm and most connective tissue fibers (Suvarna et al., 2018).

The observation and identification of collagen fibers can also be achieved using Masson's Trichrome Staining, where collagen is stained green or blue, depending on whether fast green or aniline blue is used (Al-Mahmood, 2020). Additionally, this technique highlights cell nuclei in blue-brown and cytoplasm in red.

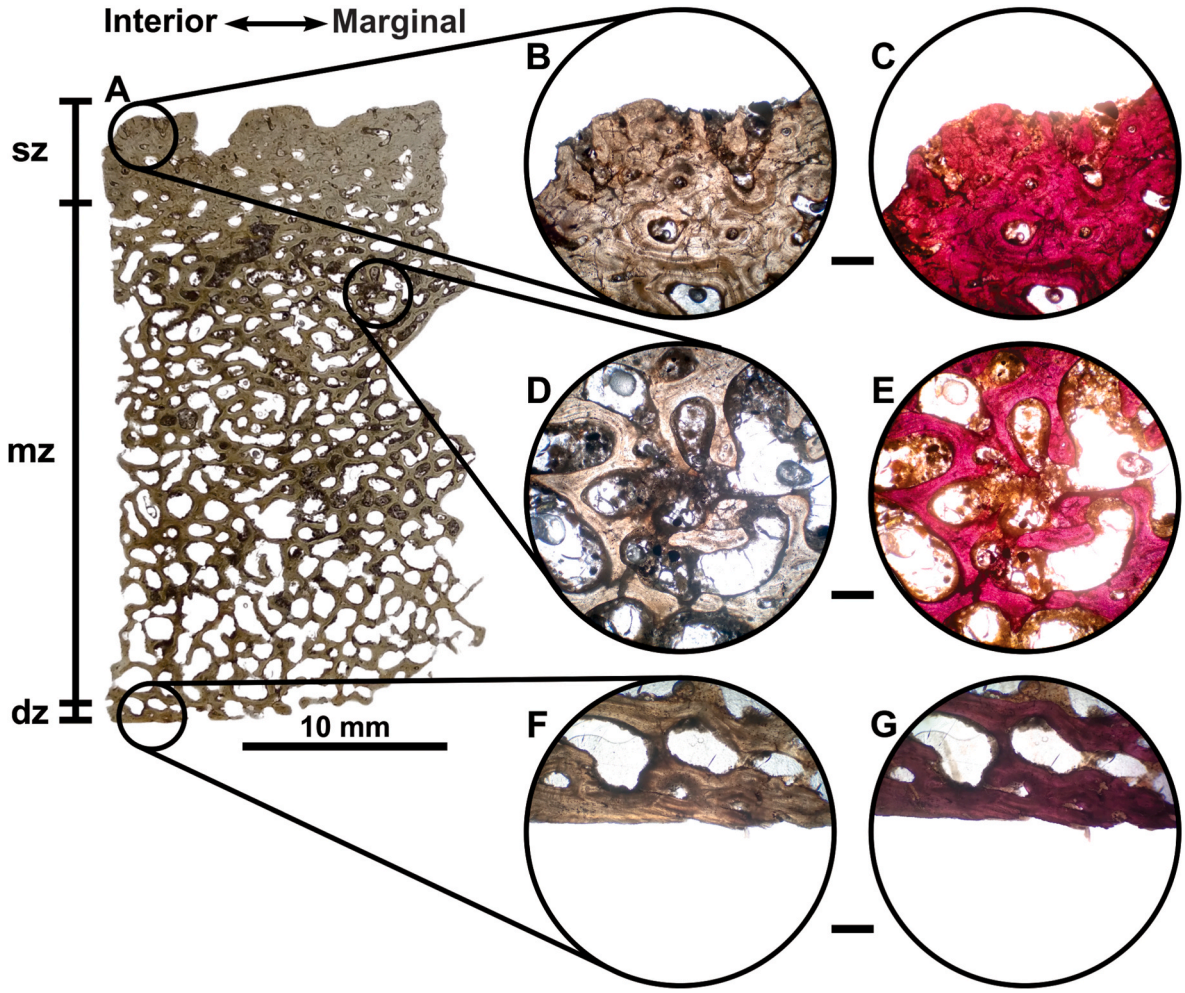

Fig. 2. H&E staining. (A) Histological section of the osteoderm of *Panochthus tuberculatus* MMCNP P2019-07. Unstained histological sections (B, D, F) and the same sections after staining (C, E, G). sz, superficial zone; mz, middle zone; dz, deep zone. Scale bar = 2 mm.

It has been established that the imbricated osteoderms of certain cingulates contain cavities filled with bone marrow (Hill, 2006; Krmpotic et al., 2015; McDonald, 2018). Bone marrow hosts precursor cells capable of differentiating into adipocytes (Delikat et al., 1993). Sudan stains have proven particularly effective in histologically identifying lipids, staining them in orange-red hues (Govan, 1944; Adams, 1969).

Coomassie blue staining is frequently used to detect proteins in polyacrylamide gels and in solution, offering a rapid, simple, and reasonably sensitive method capable of detecting protein concentrations ranging from 0.1 to 0.5 mg (Brunelle and Green, 2014). However, to date, it has not been directly applied to bone sections. Previous work by this research group on histological sections of a fossil antler of *Antifer ultra* demonstrated differential protein preservation, primarily collagen, in cortical and trabecular tissues (Brambilla et al., 2022). We propose that staining techniques could serve as rapid, non-destructive tools for evaluating the suitability of fossil samples for molecular analyses. Their most significant advantage would be their potential for straightforward implementation in laboratories worldwide, providing a standardized selection criterion when assessing large collections, particularly for determining which bones or specific regions within them might be most appropriate for biomolecular studies.

In this study, we present the results of H&E and Masson's Trichrome Staining performed on histological sections of *Panochthus tuberculatus* and *Glyptodon reticulatus*. Additionally, we report the findings from Coomassie blue staining conducted on transverse sections of osteoderms from these species. Lastly, we provide the results of lipid staining with Sudan IV (Lillie, 1969) performed on osteoderm of *G. reticulatus* that exhibited macroscopic evidence of preserved bone marrow.

2. Materials

Osteoderms of *P. tuberculatus* (MMCNP P2019-07) and *G. reticulatus* (MMCNP P2019-31), deposited in the collection of the Municipal Museum of Natural Sciences Pachamama (MMCNP), were studied. These specimens were recovered from Level A of the Camet Norte sediments, a site known for the preservation of biological material in fossils (Brambilla et al., 2024).

Additionally, two rib fragments of *Bos taurus* (LBO 056) were used as positive controls, and an osteoderm of *Doedicurus clavicaudatus* (MLS 500), from Late Pleistocene deposits in Junín with no prior reports of preserved biological material, was used as a negative control.

Histological sections were prepared from one osteoderm of *P. tuberculatus* (MMCNP P2019-07) and one of *G. reticulatus* (MMCNP P2019-31). The osteoderms were cleaned and fixed in 10 % neutral-buffered formalin for 48 h and subsequently embedded in methyl methacrylate. After polymerization (1–2 days at 37–40 °C), the samples were cured in an oven at 60 °C, following the protocol of Spijker (1978).

Thin sections, 150 μm thick, were obtained using an IsoMet low-speed saw (IsoMet 15HC, 4-inch blade, Buehler, USA). Osteoderms were sectioned perpendicular to their longest axis. Each section was mounted on a glass slide using Eukitt™ mounting medium and left

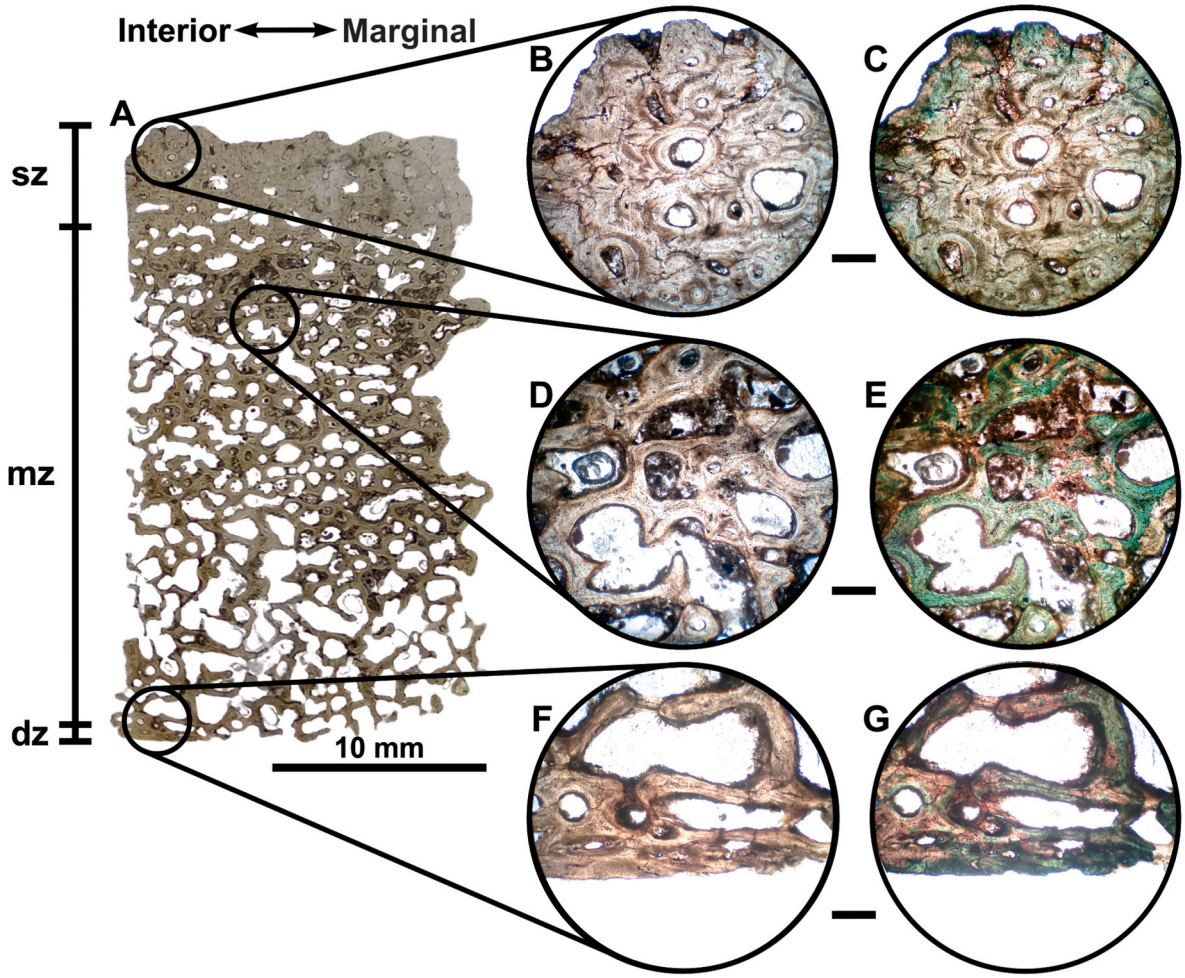

Fig. 3. Masson's Trichrome Staining. (A) Histological section of the osteoderm of *Panochthus tuberculatus* MMCNP P2019-07. Unstained histological sections (B, D, F) and after staining (C, E, G). sz, superficial zone; mz, middle zone; dz, deep zone. Scale bar = 2 mm.

overnight. Subsequently, the samples were ground to the desired thickness (~35 μm) using 600–2000 grit sandpaper, with thickness monitored periodically using a micrometer. The sections were analyzed with a Nikon Labophot microscope (20× magnification) following the methodology of Haro et al. (2020).

Coomassie blue staining. It was performed on the exposed surfaces of osteoderm sections from *P. tuberculatus* (MMCNP P2019-07) and *G. reticulatus* (MMCNP P2019-31). The sections were immersed in a Coomassie blue solution (50 % methanol, 40 % distilled water, 10 % acetic acid, 0.1 % Coomassie blue) for 30 min. They were then destained twice in a destaining solution (50 % methanol, 40 % distilled water, 10 % acetic acid) for 5 min each. Finally, the sections were air-dried at room temperature and photographed. The positive control (*Bos taurus* LBO 056) and the negative control (*Doedicurus clavicaudatus* MLS 500) were processed using the same protocol as the samples described above.

Sudan IV Staining. A cross-sectional slice of the osteoderm from *G. reticulatus* (MMCNP P2019-31), previously stained with Coomassie blue, was used for Sudan IV staining. The sample was immersed in Sudan IV 1% for 30 min, followed by washing with distilled water. Afterward, it was allowed to dry at room temperature. A positive control, consisting of a cross-section of a rib from *Bos taurus* (LBO 056), and a negative control, consisting of a sectioned osteoderm of *D. clavicaudatus*, were processed in the same manner as the sample.

H&E Staining. Histological sections were immersed in Mayer's hematoxylin solution for 10 min. They were then washed with running water for 15 min. Subsequently, two washes were performed with distilled water for 1 min each. The sections were then immersed in a 0.2 % eosin solution for 2 min. Finally, the samples were left to dry at room temperature.

Masson's Trichrome Staining. Histological sections were immersed in Weigert's ferric hematoxylin solution for 10 min, followed by washing with running water for 5 min. They were then washed with distilled water for 3 min. Next, the sections were incubated in scarlet fuchsin for 1 min, followed by washing with distilled water for 2 min. The sections were then placed in 1 % phosphomolybdic acid for 15 min and subsequently in a 2 % light green solution for 10 min. After a brief wash with distilled water, the samples were immersed in 1 % acetic acid for 3 min. Finally, the sections were left to dry at room temperature.

Histological sections were prepared from a osteoderm of *D. clavicaudatus* and a rib of *Bos taurus*, which were used as negative and positive controls, respectively, for Hematoxylin and eosin (H&E) and Masson's Trichrome Staining.

3. Results

Systematic palaeontology

Xenarthra Cope, 1889

Cingulata Illiger, 1811

Chlamyphoridae Delsuc et al., 2016

Panochthus Burmeister, 1866

Panochthus tuberculatus Owen, 1845

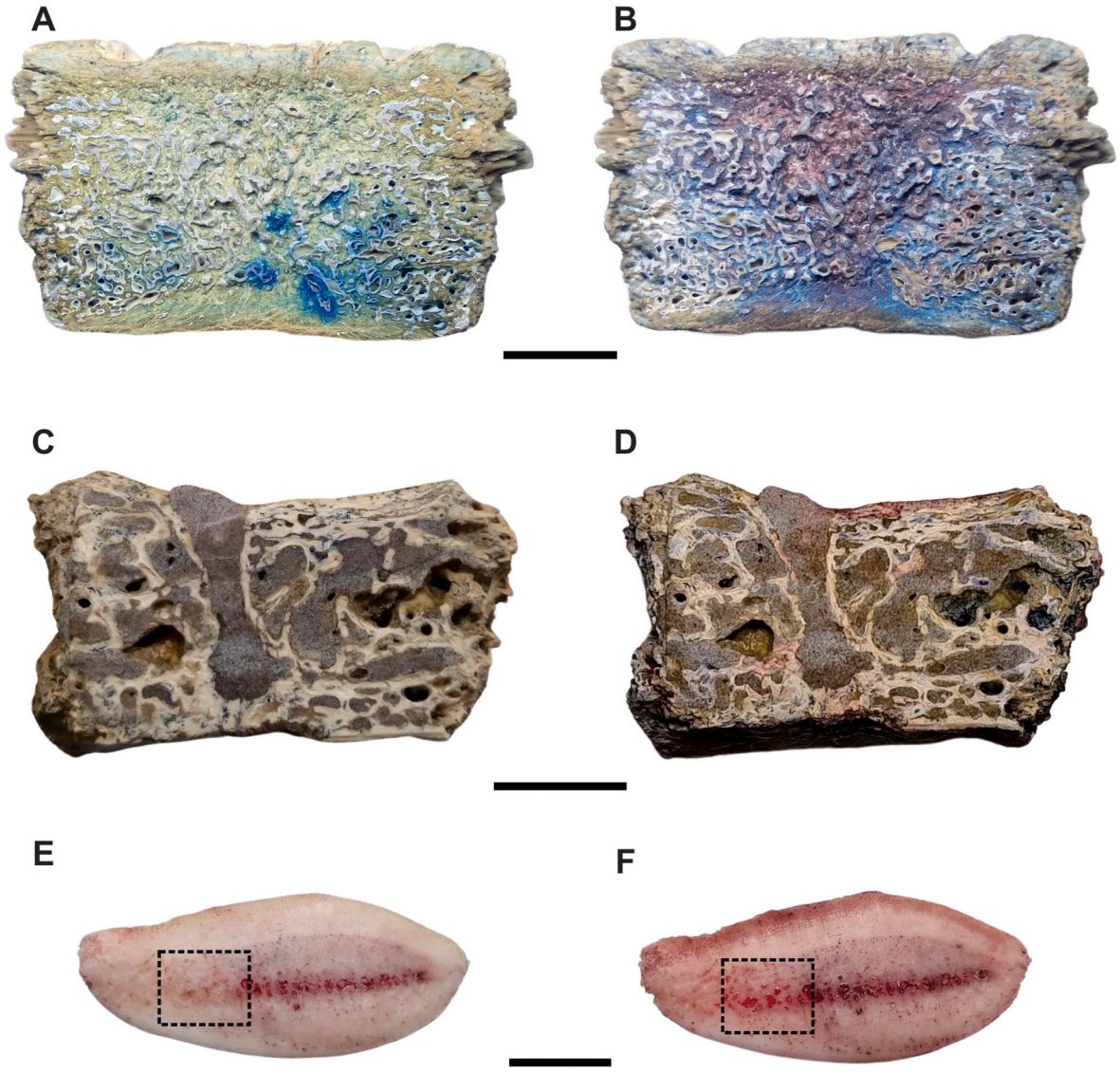

Fig. 4. Sudan IV staining. Transverse sections, unstained (A, C, E) and stained (B, D, F). Osteoderm of *Glyptodon reticulatus* MMCNP P2019-31 (A–B); osteoderm of *Doedicurus clavicaudatus* MLS 500 (C-D, negative control); rib of *Bos taurus* LBO 056 (E-F, positive control). Scale bar = 10 mm.

3.1. Coomassie blue staining

Fig. 1 shows transverse sections of the osteoderms from *P. tuberculatus* MMCNP P2019-07 alongside the positive control (*Bos taurus*) and the negative control (*Doedicurus clavicaudatus*), both before and after staining. The positive control exhibited an intense blue coloration after staining, indicating a high level of protein preservation, as expected for a modern specimen. In contrast, the negative control showed no evidence of protein preservation, as no areas retained the dye. In *P. tuberculatus* MMCNP P2019-07, protein preservation was observed mainly near the internal side and in localized regions of the outer layer of compact bone within the osteoderm (Fig. 1B).

H&E Staining. Following hematoxylin and eosin (H&E) staining, a uniform and intense red-pink coloration was observed across the bone surface in the transverse section (Fig. 2C, E, and 2G), except within the resorption areas. This indicates the preservation of organic material, possibly collagen, throughout the bone matrix. The result obtained contrasts markedly with the negative controls performed in this study, which produced a faint staining pattern and more closely resemble the results of staining conducted on modern bone (Supplementary Figs. S1 and S2).

Masson's Trichrome Staining. Green-stained bundles were observed at the inner edge of the superficial region of the osteoderm, arranged both parallel and oblique to the surface (Fig. 3C). This same green coloration was detected around the trabeculae in the intermediate zone of the osteoderm (Fig. 3E) and along the outer margin of the deep zone (Fig. 3G). In a positive control using modern bone (Suppl. Fig. S1), the bone was stained green, whereas in a negative control (Suppl. Fig. S2), no evidence of nonspecific green dye binding was observed. These findings suggest the preservation of collagen fibers in *P. tuberculatus*.

Histological Description. In a transverse section, the osteoderm of *P. tuberculatus* (MMCNP P2019-07) is predominantly composed of trabecular bone surrounded by thin layers of superficial and deep compact bone (Fig. 3A and 4A). The superficial zone (sz), formed by compact bone, exhibits an irregular appearance due to the presence of ornamental patterns on the external surface. This region shows a sparse presence of primary osteons and minimal primary bone as a result of bone remodeling processes. The intermediate zone (mz) consists of trabecular bone, characterized by resorption areas and vascular canals surrounded by concentric lamellae, reflecting a high degree of bone remodeling in this region. The deep zone (dz) also shows extensive

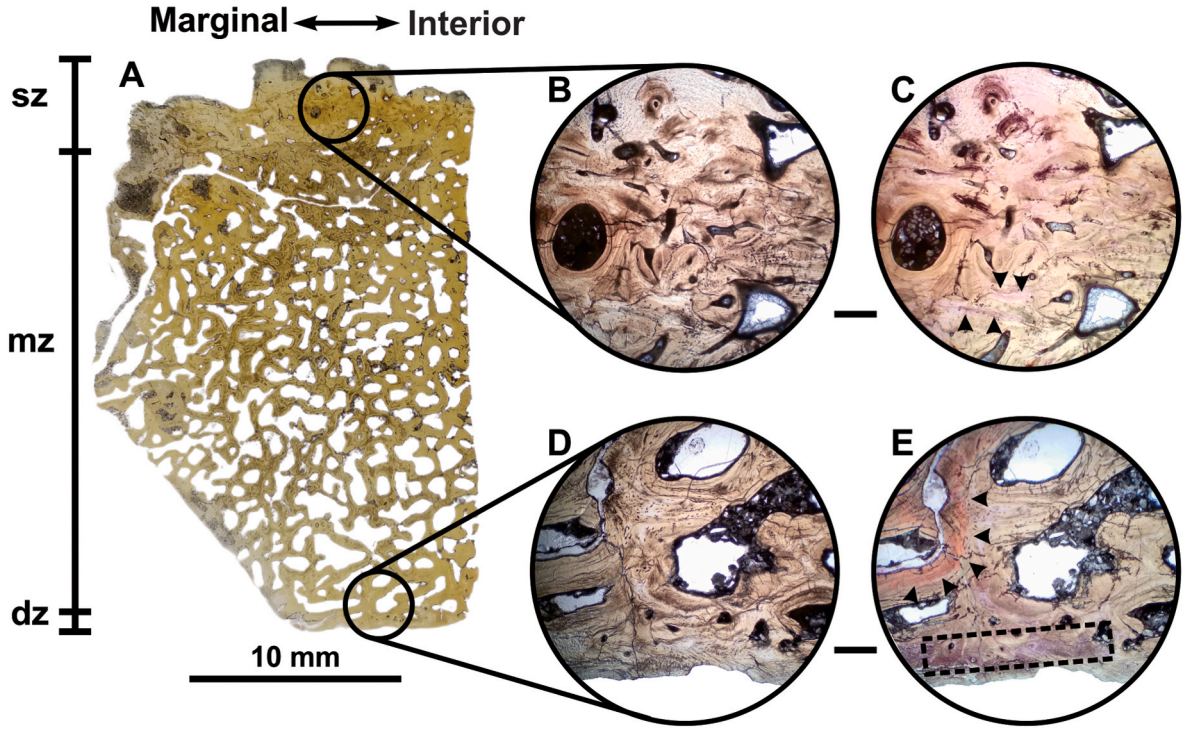

Fig. 5. H&E staining. (A) Histological section of the osteoderm of *G. reticulatus* MMCNP P2019-31. Microscopic images before staining (B, D) and after staining (C, E). Black arrows and the dotted box highlight areas of preserved connective tissue (C, E). sz, superficial zone; mz, middle zone; dz, deep zone. Scale bar = 2 mm.

remodeling, with no evidence of primary osteons. Throughout all regions, osteocyte lacunae are scarce, slightly flattened in shape, and lack preferential orientation across the entire osteoderm.

Glyptodon Owen, 1839

Glyptodon reticulatus Owen, 1845

Coomassie Blue Staining. Fig. 1 shows transverse sections of the osteoderms of *G. reticulatus* MMCNP P2019-31. Intense staining was observed in the intermediate and inner regions of the osteoderm, indicating greater protein preservation in these areas (Fig. 1D). However, it is important to note the heterogeneity of preservation, with localized spots where higher preservation appears to occur, as suggested by the staining intensity.

Sudan IV Staining. The positive control *Bos taurus* rib LBO 056) exhibited a reddish coloration primarily in the trabecular bone (dotted box, Fig. 4F), indicating the presence of lipids, as expected for a modern specimen. Similarly, for *G. reticulatus* MMCNP P2019-31, a reddish coloration was observed, primarily in the trabecular tissue toward the center of the osteoderm (Fig. 4B), indicating the preservation of lipids originating from bone marrow.

Histological description. In a transverse section, the osteoderm of *G. reticulatus* (MMCNP P2019-31) is predominantly composed of trabecular bone, surrounded by thin layers of superficial and deep compact bone (Fig. 5A and 6A). Ornamental patterns on the external surface give the superficial compact bone zone (sz) an irregular appearance. This region exhibits minimal primary bone due to osteoclastic remodeling processes, with a sparse presence of primary osteons.

The intermediate zone (mz) displays a spongy structure with resorption areas and vascular canals surrounded by concentric lamellae, reflecting a high degree of bone remodeling in this region. The deep zone (dz) contains some primary osteons. At the outer edge of this region, structures resembling Sharpey's fibers are observed, oriented perpendicularly to the surface. Overall, osteocyte lacunae are scarce in all regions, slightly flattened in shape, and lack preferential orientation throughout the osteoderm.

H&E Staining. Purple-stained bundles were observed in the center of the superficial zone (Fig. 5C). Additionally, purple staining was detected in the inner zone of the osteoderm, with patches of orange staining bordering some trabeculae in this region (indicated by the dotted box and black arrows in Fig. 5E, respectively). These results suggest the presence of preserved connective tissue fibers, albeit with a lower abundance in this material. However, the preserved regions are clearly distinguishable, standing out against the nonspecific pink background staining (Supplementary Fig. S2).

Masson's Trichrome Staining. Green-stained bundles were observed at the inner edge of the superficial region of the osteoderm, arranged in parallel and oblique orientations (Fig. 6C). The same coloration was also detected at the inner margin of the middle zone of the osteoderm (indicated by black arrows in Fig. 6E), while no staining was observed in the inner zone after the procedure (Fig. 6G). These observations suggest the presence of preserved collagen fibers, albeit to a lesser extent than in the *Panochthus* specimen, and in line with the moderate staining obtained with H&E.

4. Discussion

In this work, we observed that Coomassie blue, commonly used for protein detection in molecular biology, provides evidence of the presence of proteins in fossils, along with their spatial distribution and regions with higher preservation. Our results show that *G. reticulatus* (MMCNP P2019-31) exhibited intense staining in the middle and inner regions of the osteoderm, indicating greater protein preservation in these areas. Conversely, in *P. tuberculatus* (MMCNP P2019-07), protein conservation was mainly observed near the inner surface and localized regions of the external compact bone layer of the osteoderm.

Additionally, for the first time, we present the results of various staining techniques applied to histological sections of osteoderms from *G. reticulatus* and *P. tuberculatus*. Hematoxylin and eosin (H&E) staining revealed the preservation of connective tissue fibers in both the central area of the superficial zone and the inner zone of the osteoderm of *G. reticulatus* (MMCNP P2019-31). For *P. tuberculatus* (MMCNP P2019-

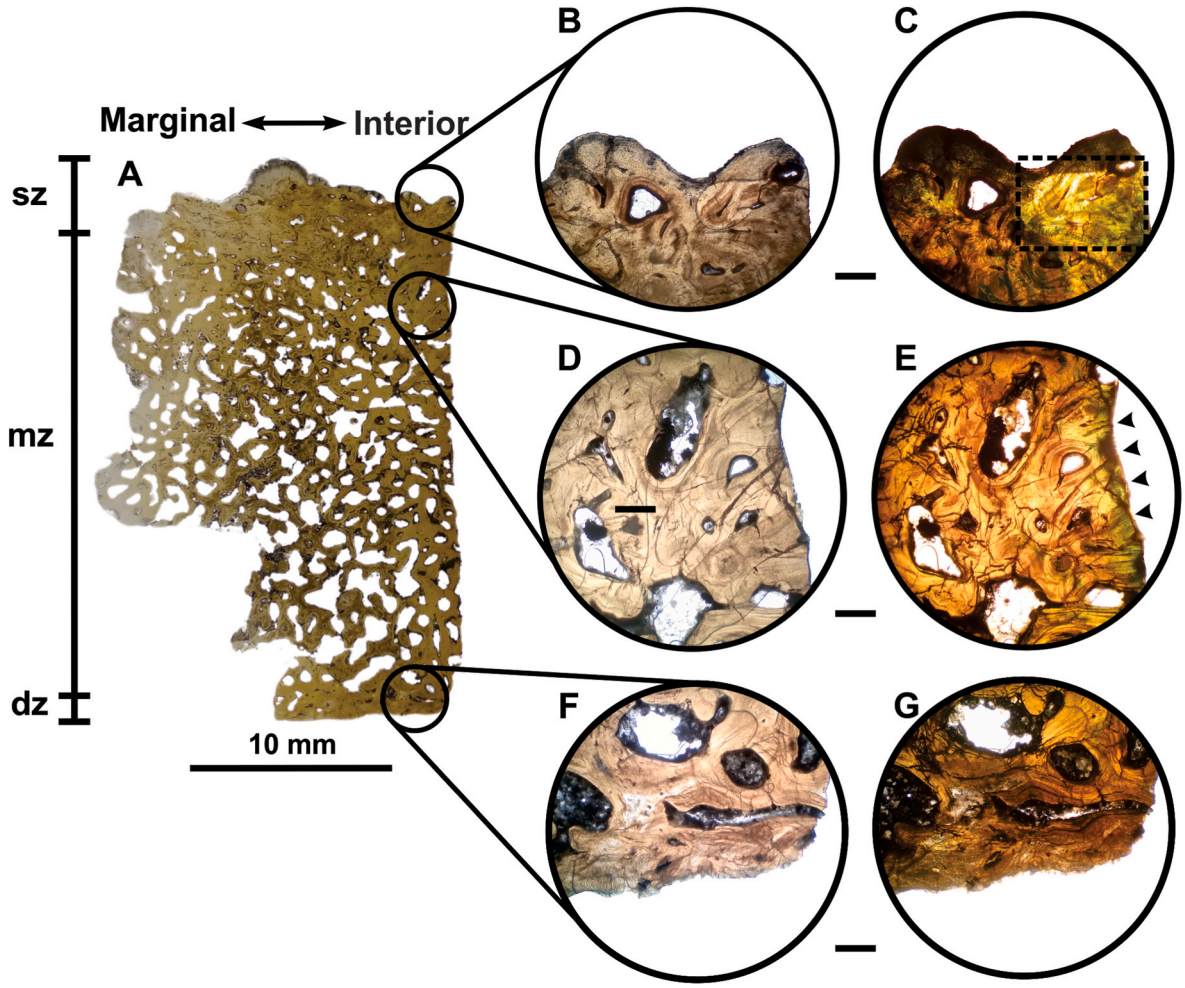

Fig. 6. Masson's Trichrome Staining. (A) Histological section of the osteoderm of *G. reticulatus* MMCNP P2019-31. Microscopic images before staining (B, D, F) and after staining (C, E, G). Black arrows and the dotted box highlight areas of preserved collagen fibers. sz, superficial zone; mz, middle zone; dz, deep zone. Scale bar = 2 mm.

07), conservation was uniformly observed throughout the entire osteoderm.

Similarly, Masson's Trichrome Staining demonstrated collagen fiber preservation at the inner margin of the superficial region and the inner edge of the middle zone in *G. reticulatus* (MMCNP P2019-31), while in *P. tuberculatus* (MMCNP P2019-07), the technique showed greater preservation in the middle and deeper regions compared to the superficial zone.

Upon comparative analysis of two fossil bone samples, *P. tuberculatus* exhibits intense hematoxylin-eosin (H&E) staining, whereas *G. reticulatus* shows a markedly fainter and localized stain. Although both samples demonstrate evidence of organic matter preservation, the disparity in staining intensity suggests that, when evaluating multiple materials with preserved organic content, it would be prudent to prioritize samples displaying stronger staining, over those with weaker signals, due to their superior degree of preservation.

We performed positive and negative controls to validate our results. In the positive controls, H&E staining produced a strong red-pink coloration throughout the bone, demonstrating its effectiveness in staining organic components within the bone matrix (Supplementary Fig. S1). In contrast, the negative control showed only a very faint and uniform pink background across the entire histological section (Supplementary Fig. S2). For this reason, areas with positive preservation of organic material in the fossils were observed as regions of intense coloration, standing out against the faint pink background. Preservation was evident throughout the bone tissue and frequently concentrated within the lamellae. This pattern highlights the deposition and organization of the bone's lamellar structure. The staining of lamellar structures suggests that organic material, such as collagen, remains sufficiently intact to interact with the dye.

Similarly, the controls performed for Masson's Trichrome Staining showed that, in the positive controls, the bone tissue was stained green, highlighting its effectiveness in revealing the organic components. In contrast, staining performed on a negative control did not produce any nonspecific green coloration. Accordingly, we reliably observed that this staining produced distinctly green areas in the analyzed fossils, confirming the presence of organic material in these specimens and in specific regions of the bone.

Moreover, Sudan IV staining revealed abundant red coloration, primarily in the trabecular tissue at the center of the osteoderm in *G. reticulatus* (MMCNP P2019-31), indicating the preservation of lipids from bone marrow. This finding highlight that not only proteins and DNA can be preserved but also lipids from bone marrow, opening new research avenues focused on the extraction of these compounds for stable isotope analysis. This approach could be employed to cross-validate stable isotope results from lipids with those obtained from collagen purification, ensuring robust data by analyzing components of different biochemical nature, lipidic and proteic, from the same sample.

Additionally, the presence of lipids in Late Pleistocene materials is highly novel and raises the possibility that not only the bone marrow, evidenced by lipid preservation, but also white and red blood cells might be preserved in in bone marrow. Such discoveries could enable future

morphological analyses of extinct organisms.

This study did not investigate the detection limits of each staining method. Instead, we focused on the presence or absence of color and its intensity in positive cases. This approach is useful for comparing the abundance of organic material in bone samples, enabling a comparative analysis. Future research could correlate the concentration of specific molecules and macromolecules, as determined by other analytical methods, with the observed staining intensity.

5. Conclusions

Fossils can retain original organic material, offering a valuable resource for innovative research in paleontology and the study of these molecules will expand our understanding of unresolved aspects of ancient life.

The staining techniques applied in this work demonstrate their potential for use in both histological sections and direct fossil samples. This approach allows for the rapid identification of preserved organic material in fossils and the spatial localization of preservation areas.

Our results reveal that preservation within fossils is heterogeneous, with some regions exhibiting greater conservation than others. Using staining techniques, researchers can specifically target the best-preserved areas for future molecular analyses, such as the extraction of lipids, proteins, or DNA.

CRediT authorship contribution statement

Damián A. Ibarra: Writing – original draft, Investigation. **Luciano Brambilla:** Writing – review & editing, Writing – original draft, Validation, Supervision, Project administration, Methodology, Investigation, Conceptualization. **Pablo Straccia:** Writing – review & editing, Validation, Resources. **Rubén D. Scian:** Writing – review & editing, Validation, Resources. **Lucas R. Brun:** Writing – review & editing, Validation, Supervision, Project administration, Conceptualization.

Declaration of competing interest

The authors declare that they have no known competing financial interests or personal relationships that could have appeared to influence the work reported in this paper.

Acknowledgments

We would like to express our gratitude to José María Marchetto and to the Legado del Salado Museum in the city of Junín. We also extend our thanks to the Municipal Museum of Natural Sciences “Pachamama” of Camet Norte (Buenos Aires) and its staff, as well as to the Center for Identity, Environment, and Heritage Studies Pachamama (CECIAPP, Buenos Aires).

Appendix A. Supplementary data

Supplementary data to this article can be found online at https://doi.org/10.1016/j.jsames.2025.105454.

Data availability

Data will be made available on request.

References

Adams, C.W.M., 1969. Lipid histochemistry. Adv. Lipid Res. 1–62. https://doi.org/10.1016/b978-0-12-024907-7.50008-7.

Al-Mahmood, S.S., 2020. Improving light microscopic detection of collagen by trichrome stain modification. Iraqi J. Vet. Sci. 34 (2), 273–281.

Anderson, L.A., 2022. Biomolecular histology as a novel proxy for ancient DNA and protein sequence preservation. Ecol. Evol. 12 (12), e9518.

Asakura, Y., Da Costa, P.V.L.G., Oliveira, E.V., Da Silva, J.L.L., 2017. Comparative paleohistology in osteoderms of Pleistocene *Panochthus* sp. Burmeister, 1886 and *Neuryurus* sp. (Xenarthra, Glyptodontidae). C. R. Palevol 16 (7), 795–803.

Boatman, E.M., Goodwin, M.B., Holman, H.Y.N., Fakra, S., Zheng, W., Gronsky, R., Schweitzer, M.H., 2019. Mechanisms of soft tissue and protein preservation in *Tyrannosaurus rex*. Sci. Rep. 9 (1), 15678.

Boatman, E.M., Goodwin, M.B., Holman, H.Y., Fakra, S., Schweitzer, M.H., Gronsky, R., Horner, J.R., 2014. Synchrotron chemical and structural analysis of *Tyrannosaurus rex* blood vessels: the contribution of collagen hypercrosslinking to tissue longevity. Microsc. Microanal. 20 (S3), 1430–1431.

Brambilla, L., López, P., Ibarra, D., Brun, L., 2022. Tinción histológica revela la localización de proteínas preservadas en una asta de *Antifer ultra*. PE-APA 22 (2), 11.

Brambilla, L., Ibarra, D.A., Barboza, M.C., Bresso, E.G., Rosano, G., Pérez, G., Straccia, P., Scian, R.D., Brun, L.R., 2024. Mitochondrial genome of *Neuryurus rudis* (Xenarthra, Cingulata); contribution to phylogeny and origin of glyptodonts. Gene. https://doi.org/10.1016/j.gene.2024.149059.

Brunelle, J.L., Green, R., 2014. Coomassie blue staining. Methods Enzymol. 541, 161–167. Academic Press.

Burmeister, G., 1866. Lista de mamíferos fósiles del terreno diluviano. An. Museo Publico Buenos Aires 1, 121–300.

Cadena, E.A., Schweitzer, M.H., 2012. Variation in osteocytes morphology vs bone type in turtle shell and their exceptional preservation from the Jurassic to the present. Bone 51 (3), 614–620.

Colleary, C., O'Reilly, S., Dolocan, A., Toyoda, J.G., Chu, R.K., Tfaily, M.M., et al., 2022. Using macro and microscale preservation in vertebrate fossils as predictors for molecular preservation in fluvial environments. Biology 11 (9), 1304.

Cope, E.D., 1889. The Edentata of North America. Am. Nat. 23, 657–664. https://doi.org/10.1086/274985.

Da Costa, P.V.L.G., Victer, G.D., Porpino, K.D.O., Bergqvist, L.P., 2012. Osteoderm histology of Late Pleistocene cingulates from the intertropical region of Brazil. Acta Palaeontol. Pol. 59 (3), 543–552.

Delikat, S., Harris, R.J., Galvani, D.W., 1993. IL-1 beta inhibits adipocyte formation in human long-term bone marrow culture. Exp. Hematol. 21 (1), 31–37.

Delsuc, F., Gibb, G.C., Kuch, M., Billet, G., Hautier, L., Southon, J., et al., 2016. The phylogenetic affinities of the extinct glyptodonts. Curr. Biol. 26 (4), 155–156.

Govan, A.T., 1944. Fat-staining by Sudan dyes suspended in watery media. J. Pathol. Bacteriol. 56 (2), 262–264.

Haro, J.A., Brambilla, L., Brun, L.R., Ibarra, D.A., Zuccari, J.I., Marchetto, J.M., 2020. Histology of 'uncommon'osteoderms of *Glyptodon reticulatus* Owen, 1845 (Mammalia, Xenarthra) from the late Pleistocene of Argentina and its systematic and developmental implications. J. S. Am. Earth Sci. 101, 102613.

Hill, R.V., 2006. Comparative anatomy and histology of xenarthran osteoderms. J. Morphol. 267 (12), 1441–1460.

Illiger, C., 1811. In: Salfeld, C. (Ed.), Prodromus systematis mammalium et avium; additis terminis zoographicis utriusque classis, eorumque versione germanica, p. 301. Berlin.

Krmpotic, C.M., Ciancio, M.R., Carlini, A.A., Castro, M.C., Scarano, A.C., Barbeito, C.G., 2015. Comparative histology and ontogenetic change in the carapace of armadillos (Mammalia: Dasypodidae). Zoomorphology 134, 601–616.

Lillie, R.D., 1969. HJ Conn's Biological stains: a handbook on the nature and uses of the dyes employed in the biological laboratory. In: 8th. Williams & Wilkins, Baltimore, p. 6. 65-66, 99-101, 407-408.

Luna, C.A., Cerda, I.A., Zurita, A.E., Gonzalez, R., Prieto, M.C., Mothé, D., Avila, L.S., 2018. Distinguishing Quaternary glyptodontine cingulates in South America: how informative are juvenile specimens? Acta Palaeontol. Pol. 63 (1), 159–170.

McDonald, H.G., 2018. An overview of the presence of osteoderms in sloths: implications for osteoderms as a plesiomorphic character of the Xenarthra. J. Mamm. Evol. 25 (4), 485–493.

Owen, R., 1839. Description of a Tooth and Part of the Skeleton of the *(Glyptodon)*, a Large Quadruped of the Edentate Order, to Which Belongs the Tessellated Bony Armour Figured by Mr Clift in His Memoir on the Remains of the *Megatherium*, Brought to England by Sir Woodbine Parish, F.G.S, vol. 3. Proceedings of the Geological Society of London, pp. 108–113.

Owen, R., 1845. Descriptive and Illustrated Catalogue of the Fossil Organic Remains of Mammalia and Aves Contained in the Museum of the Royal College of Surgeons of London. Royal College of Surgeons of England, London, p. 391.

San Antonio, J.D., Schweitzer, M.H., Jensen, S.T., Kalluri, R., Buckley, M., Orgel, J.P., 2011. Dinosaur peptides suggest mechanisms of protein survival. PLoS One 6 (6), e20381.

Schweitzer, M.H., Suo, Z., Avci, R., Asara, J.M., Allen, M.A., Arce, F.T., Horner, J.R., 2007a. Analyses of soft tissue from *Tyrannosaurus rex* suggest the presence of protein. Science 316 (5822), 277–280.

Schweitzer, M.H., Wittmeyer, J.L., Horner, J.R., 2007b. Soft tissue and cellular preservation in vertebrate skeletal elements from the Cretaceous to the present. Proc. Biol. Sci. 274 (1607), 183–197.

Schweitzer, M.H., Zheng, W., Cleland, T.P., Bern, M., 2013. Molecular analyses of dinosaur osteocytes support the presence of endogenous molecules. Bone 52 (1), 414–423.

Schweitzer, M.H., Zheng, W., Organ, C.L., Avci, R., Suo, Z., Freimark, L.M., et al., 2009. Biomolecular characterization and protein sequences of the Campanian hadrosaur *B. canadensis*. Science 324 (5927), 626–631.

Spijker, H.J., 1978. A procedure for obtaining thin sections of undercalcified bone biopsies embedded in methyl methacrylate. Microsc. Acta 81 (1), 17–26.
Suvarna, K.S., Layton, C., Bancroft, J.D., 2018. Bancroft's Theory and Practice of Histological Techniques E-Book. Elsevier health sciences.
Wolf, D., Kalthoff, D.C., Sander, P.M., 2012. Osteoderm histology of the Pampatheriidae (Cingulata, Xenarthra, Mammalia): implications for systematics, osteoderm growth, and biomechanical adaptation. J. Morphol. 273 (4), 388–404.